Magnetic dynamic phase generated by spin currents

Jiexuan He and Shufeng Zhang
Department of Physics, University of Arizona, Tucson, Arizona 85721, USA
(Received 24 May 2008; revised manuscript received 24 June 2008; published 24 July 2008)

A large nonequilibrium spin-polarized current can induce a magnetization dynamic phase (ferrodynamics) when the static uniform magnetization becomes unstable. We quantitatively determine the transport and magnetic properties of the ferrodynamic phase. The scaling exponents near the critical current are analyzed via numerical simulations. We further propose the existence of the spin electric-motive force in the ferrodynamic phase.

DOI: 10.1103/PhysRevB.78.012414 PACS number(s): 85.75.−d, 72.25.Pn, 75.40.Gb, 75.70.Kw

I. INTRODUCTION

One of the emerging subjects in magnetoelectronics is the magnetization dynamics driven by a spin-polarized current.[1,2] In magnetic spin valves and tunnel junctions, a sufficiently large current could lead to precession[3] or reversal[4,5] of one of the magnetic layers. In a single ferromagnetic layer or wire, a large spin-polarized current may drive domain walls into motion[6] and generate spin waves.[7,8] These discoveries have fueled a new direction of research in current-controlled manipulation of magnetization dynamics for memory technology application.[9–11]

Up until now, theoretical and experimental efforts were focused on the critical values of the current for domain-wall motion and for spin-wave excitations. When there is a preexisting domain wall in a nanowire, a critical value of the current I_{c1} is required to overcome the pinning potential in order to move the domain wall.[12,13] If the nanowire is initially uniformly magnetized, i.e., there is no domain wall, a second and larger critical value of the current I_{c2} is needed to destabilize the uniform magnetization. A further increase in the current will lead to chaotic magnetization dynamics.[14,15] Although the existence of this second critical current I_{c2} has already been predicted by a number of papers,[16–20] the physical properties near the critical current has never been investigated. In this Brief Report, we determine the fundamental excitations of a uniform magnetic nanowire induced by the spin current. We define the magnetization dynamics above I_{c2} as a ferrodynamic phase which can be characterized by the critical exponents at the transition region close to I_{c2}. We further predict an induced electromotive force (emf) at the ferrodynamic phase.

II. MODEL

We start with the equation of motion for the magnetization in the presence of the current,[21,22]

$$\frac{\partial \mathbf{m}}{\partial t} = -\gamma \mathbf{m} \times \mathbf{H}_{\text{eff}} + \alpha \mathbf{m} \times \frac{\partial \mathbf{m}}{\partial t} - jb\mathbf{m} \times \left(\mathbf{m} \times \frac{\partial \mathbf{m}}{\partial x} \right) - jc\mathbf{m} \times \frac{\partial \mathbf{m}}{\partial x}, \tag{1}$$

where $\mathbf{m}=\mathbf{M}/M_s$ is the magnetization vector, γ is the gyromagnetic ratio, $\mathbf{H}_{\text{eff}}$ is the effective field, α is the Gilbert damping parameter and M_s is the saturation magnetization. The last two terms describe the adiabatic and nonadiabatic spin torques, respectively, where j is the current density in the direction of $\hat{e}_x$, $b=P\mu_B/eM_s$ and $c=\xi b$, P is the spin polarization and ξ is a phenomenological constant.[21]

III. LINEAR INSTABILITY

The critical current density j_{c2} can be immediately obtained by the conventional linear instability analysis. Consider a small deviation of the uniform magnetization, $\mathbf{m}(x,t)=\hat{e}_x+\delta\mathbf{m}\exp[i\omega(k)t-ikx]$ where $\delta\mathbf{m}$, k and $\omega(k)$ are, respectively, the amplitude (small vector perpendicular to $\hat{e}_x$), wave vector and frequency of spin wave. Since we assume the wire is infinitely long and the boundary effect is discarded, $\delta\mathbf{m}$ can be treated as a spatially-independent constant. By placing $\mathbf{m}(x,t)$ into Eq. (1) and carrying out the linear instability analysis, we find

$$\begin{bmatrix} -i(\omega+jbk) & f_1 \\ f_2 & -i(\omega+jbk) \end{bmatrix} \begin{bmatrix} \delta m_y \\ \delta m_z \end{bmatrix} = 0, \tag{2}$$

where we have defined $f_1=-\gamma(J_{ex}k^2+H_1)-i(\alpha\omega+jck)$ and $f_2=\gamma(J_{ex}k^2+H_2)+i(\alpha\omega+jck)$, where $H_1=H_e+H_k+4\pi M_s$ and $H_2=H_e+H_k$, where H_e and H_k are the external field and the anisotropy field along the wire; J_{ex} is the exchange constant. By calculating the determinant of the above secular equation, one could find the critical current $j_c(k)$ at the onset of instability (Im $\omega=0$)

$$j_c(k) = \frac{\gamma}{k(b-c/\alpha)} \sqrt{(J_{ex}k^2+H_1)(J_{ex}k^2+H_2)}. \tag{3}$$

By minimizing $j_c(k)$ with respect to k, i.e., $\partial j_c/\partial k=0$, we find the minimum critical current density j_{c2} is

$$j_{c2} = \gamma\sqrt{J_{ex}}(\sqrt{H_1}+\sqrt{H_2})/|b-c/\alpha|. \tag{4}$$

Interestingly, only a single spin wave with frequency $\omega_c=j_{c2}(c/\alpha)(H_1H_2/J_{ex}^2)^{1/4}$ is excited at j_{c2}. One notes that j_{c2} is infinite when $\xi\equiv c/b=\alpha$. The lack of spin-wave excitations in this case can be traced back to Eq. (1): When one makes a Galilean transformation, $x'=x-jbt$ and $t'=t$, Eq. (1) becomes a usual LLG equation without the spin torque terms. Thus, the spin-wave excitations are prohibited when $\xi=\alpha$ as expected for a Galilean invariance system. The exact relation

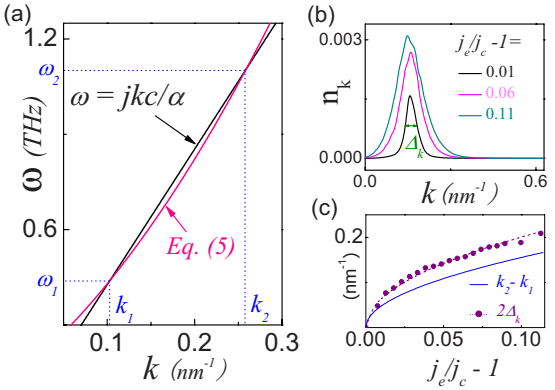

FIG. 1. (Color online) (a) The spin-wave dispersion relation [Eq. (5)] plotted with a fixed current density $j/j_{c2}=1.1$ [the red (dark gray) curve], and the part of black line [$\omega(k)=-jkc/\alpha$] above the red curve indicates the region of instability. (b) Spin-wave distribution n_k calculated from Eq. (7). (c) The spectrum width $2\Delta_k$ and the analytical result $\Delta_k^0 \equiv k_2 - k_1$ derived from Fig. 1(a).

between b and c has been the subject of the theoretical controversy,[23–25] but in general $\xi \neq \alpha$. We set $\xi=2\alpha$ for the rest of the Brief Report.

IV. SPIN-WAVE DISTRIBUTION

When the current density is larger than j_{c2}, the excited spin-wave frequency expands from a single value to a finite range. The secular equation corresponding to Eq. (2) leads to the spin-wave dispersion relation

$$\omega(k) = -jbk + \gamma\sqrt{(J_{ex}k^2 + H_1)(J_{ex}k^2 + H_2)}, \tag{5}$$

where the first term on the right-hand side is known as the Doppler shift.[17] In addition, the spin wave becomes unstable when Im $\omega<0$, i.e.,

$$\omega(k) < -jk\frac{c}{\alpha}. \tag{6}$$

For illustration, we plot both Eq. (5) and $\omega(k)=-jk(c/\alpha)$ in Fig. 1(a) with $j/j_{c2}=1.1$. The spin waves with wave vector k in the range $k_1<k<k_2$ are all excitable since they satisfy both Eqs. (5) and (6). To describe the ferrodynamic phase for $j>j_{c2}$, we first quantitatively determine the number of the spin waves excited by the current by using the micromagnetic simulation. The wire is chosen to be 4 μm in length, 20 nm in width and 5 nm in thickness. We have used open boundary conditions in the directions of width and thickness, but used the periodic boundary in the length direction. The mesh size is taken as $2\times2\times5$ nm^3. To reduce the computation time we replace the magnetostatic interaction by the demagnetization field perpendicular to the plane for most of the numerical results. The full consideration of the magnetostatic interaction for a few selected simulations reveals the same qualitative conclusions discussed below. We start with the magnetization being initially magnetized along the wire with small random fluctuations. The magnetization evolves with time according to Eq. (1). After a few nanoseconds, we start to record the magnetization vector $\mathbf{m}(x,t)$. The degree of initial nonuniformity of magnetization affects the time needed to excite the spin waves. However, the results presented in the present work are obtained at the long-time limit where the average physical properties do not depend on the initial condition.

When the current density is below the critical value j_{c2}, $\mathbf{m}(x,t)$ always returns $\mathbf{m}=\mathbf{e}_x$, i.e., the uniform magnetization is the only stable mode. Once $j>j_{c2}$, small-amplitude spin waves with well-defined wavelength and frequency are generated, indicating the ferromagnetic instability. The number of the spin wave n_k is

$$n_k = \lim_{T\to\infty}\frac{1}{T}\int_0^T dt|\mathbf{m}_\perp(k,t)|^2, \tag{7}$$

where $\mathbf{m}_\perp(k,t)$ is the Fourier transformation of the perpendicular component of magnetization $\mathbf{m}_\perp(x,t)$. In Fig. 1(b) we show the spin-wave distribution for three different current densities. The spectrum width Δ_k, which is defined as the width at the half maximum, displays a scaling relation, $\Delta_k \sim (j-j_c)^\nu$. The exponent ν is not universal; it depends on the applied magnetic field. It is interesting to compare $2\Delta_k$ with the analytical result $\Delta_k^0=k_2-k_1$. As shown in Fig. 1(c), $2\Delta_k$ is generally larger than Δ_k^0, indicating the importance of the interaction among the excited spin waves.

We have noted that the simulation yields some complicated structures such as vortex and antivortex pairs. These states are formed due to the strong spin-wave interaction. Nakatani *et al.*[15] have recently analyzed the properties of these states in great detail by using a different boundary condition. Here we neglect these ultrahigh energy excitations since they have a very short lifetime and contribute insignificantly to the spin-wave distribution.

V. ORDER PARAMETERS

Next we calculate the saturation magnetization above the critical point. The current induced excitations could cause the fluctuations of the instantaneous magnetization $m_s(t) = |\int_0^L dx\mathbf{m}(x,t)/L|$. The inset of Fig. 2(a) shows two examples of $m_s(t)$ for different current density. The order parameter is then defined by

$$m_s = \lim_{T\to\infty}\frac{1}{T}\int_0^T m_s(t)dt. \tag{8}$$

In Fig. 2(a), we have fitted the order parameter by the scaling relation $1-m_s=C_0(j/j_{c2}-1)^{\beta(H)}$ for several different magnetic fields which are applied in x direction. The exponent $\beta(H)$ depends on the field. The external field dependence of the exponent is shown in Fig. 2(a). The reduction of the exponent for the increase in the field is due to suppression of the fluctuation of $m_s(t)$, similar to the thermally driven phase transition. The susceptibility, $\chi \equiv (\partial m_s/\partial H_e)$, does not show a single exponent scaling. This is because the critical current, see Eqs. (3) and (4), depends on the field and one could find that χ scales with $C_1(j-j_c)^{\beta-1}+C_2(j-j_c)^\beta \ln(j-j_c)$, where C_1 and C_2 are noncritical coefficients.

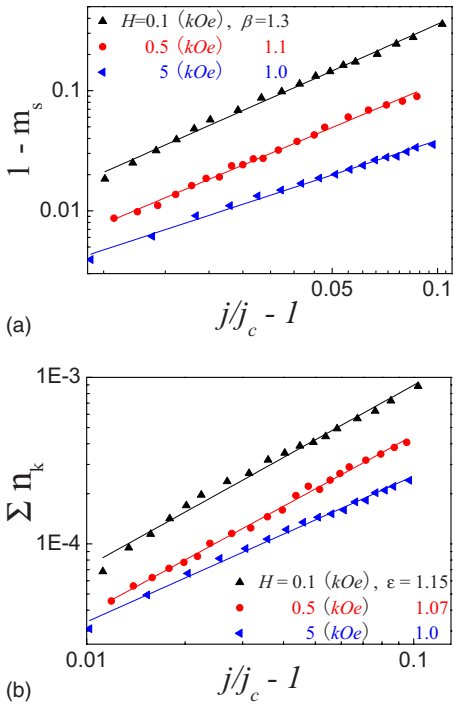

FIG. 2. (Color online) (a) Simulation results of the saturation magnetization m_s calculated from Eq. (8) as a function of current density with three different external fields. (b) The total number of the spin wave Σn_k calculated from Eq. (7) as a function of current density with three different external fields.

We also calculate the time-averaged magnetization in the direction of the magnetic field by $\langle m_x \rangle = 1 - \int dk n_k$. As shown in Fig. 2(b), we find the exponent ε is slightly different from that of the order parameter. We attribute this difference to the "frequency filtering" of the fast Fourier transform calculation of $\mathbf{m}_\perp(k,t)$: Shot-noise-like wall/vortex-pair excitations have been partially filtered in the transformation while m_s includes such higher-energy excitations.

VI. SPIN ELECTROMOTIVE FORCES

Accompanying with the phase transition from the uniformly magnetized state to the ferrodynamic state, an emf appears.[23–28] The spin emf is the reaction of the magnetization dynamics to the electric current. In magnetic spin valves, the magnetization precession can create a spin current of the conduction electron known as spin pumping.[29] Similarly, the domain-wall motion can also produce a spin current which is termed as the spin emf. We show below that the spin waves generated by the current lead to an induced voltage. To obtain the induced emf, let us consider the rate of energy (density) change in the magnetic wire from Eq. (1),

$$\frac{\partial E}{\partial t} = -\alpha\gamma M_s |\mathbf{m}\times\mathbf{H}_{\text{eff}}|^2 - b' j M_s \left(\mathbf{H}_{\text{eff}}\cdot\frac{\partial \mathbf{m}}{\partial x}\right) + c' j M_s \left[\mathbf{H}_{\text{eff}}\cdot\left(\mathbf{m}\times\frac{\partial \mathbf{m}}{\partial x}\right)\right], \tag{9}$$

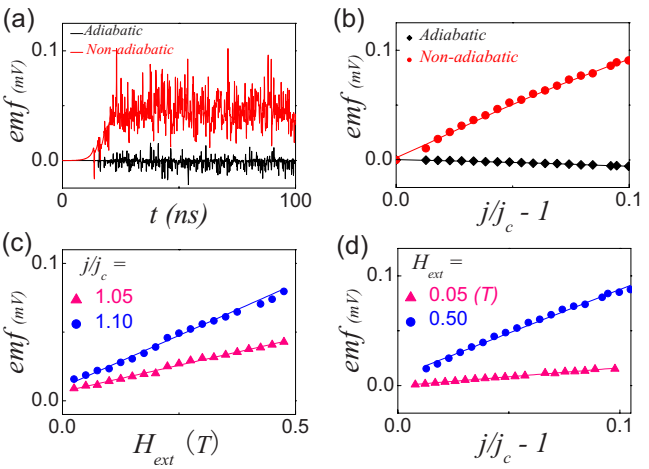

FIG. 3. (Color online) Time-dependent (a) and time-averaged (b) spin emf generated by the adiabatic (black) and nonadiabatic (red) torques, where $H_e = 0.5T$ and $j/j_{c2} = 1.05$: Total spin emf as functions of fields (c) and currents (d).

where the first term on the right-hand side represents the energy dissipated into the background (i.e., lattices), and the second and third terms are the energy pumped into the magnetic system by the current, where $b' = (1+\alpha\xi)b$ and $c' = (\xi - \alpha)b$. Conversely, we can interpret the second and third terms as a power loss of the conduction electrons. If we define the induced emf by relating $j\varepsilon_{\text{emf}}$ to this power loss in Eq. (9), we have

$$\varepsilon_{\text{emf}} = \int dx \frac{\partial E_{\mathbf{m}}}{j\,\partial t} = -b' \int dx M_s \left(\mathbf{H}_{\text{eff}}\cdot\frac{\partial \mathbf{m}}{\partial x}\right) + c' \int dx M_s \left[\mathbf{H}_{\text{eff}}\cdot\left(\mathbf{m}\times\frac{\partial \mathbf{m}}{\partial x}\right)\right]. \tag{10}$$

A similar expression has been previously made by Saslow.[26] The essential physics of the induced emf is same as the spin pumping: The dynamics of the magnetization leads to an induced spin current that generates an additional voltage via spin accumulation.[29] Note from Eq. (10) that the emf has both adiabatic and nonadiabatic contributions.

To estimate the emf generated in the ferrodynamic phase, we expand $\mathbf{m}(x,t)$ in Eq. (1) near $\mathbf{m} = \mathbf{e}_x$ and only keep the second order in m_y and m_z,

$$\mathbf{m}(x,t) = \left[1 - \frac{1}{2}(m_y^2 \sin^2\Omega + m_z^2 \cos^2\Omega)\right]\mathbf{e}_x + m_y \sin\Omega \mathbf{e}_y + m_z \cos\Omega \mathbf{e}_z, \tag{11}$$

where $\Omega = \omega(k)t - kx$. By placing Eq. (11) into Eq. (10), we find

$$\varepsilon = b' \int dx M_s f(m_y^2, m_z^2) \sin 2\Omega + c' \int dx M_s (J_{ex}k^2 + H_2 + 4\pi M_s \cos^2\Omega) k m_y m_z, \tag{12}$$

where $f(m_y^2, m_z^2)$ is a function of m_y^2 and m_z^2 which do not explicitly depend on t and x. The first term on the right-hand side is the contribution from the adiabatic torque; the time

average is approximately zero due to the oscillatory function $\sin 2\Omega$. In the ordinary current-driven domain-wall motion, the emf from the adiabatic torque[23] is generally nonzero when a domain wall moves across a voltage probe. Here we can treat ferrodynamic phase as multiple moving domain walls with equal numbers of the head-to-head and tail-to-tail walls passing through a voltage probe. Thus the positive and negative signals of the induced emf are averaging to zero.

The second term in Eq. (12) is proportional to the nonadiabatic torque which is not zero upon time and spatial averaging. Therefore, the emf generated in the ferrodynamic phase is mainly from the nonadiabatic component of spin transfer between conduction electrons and local moments. We confirm the above analysis by numerically calculating the emf from Eq. (10). While both terms in Eq. (10) show strong fluctuations due to the presence of nonlinear wall/vortex-pair excitations as shown in Fig. 3(a), the average emf is clearly dominated by the nonadiabatic torque; see Fig. 3(b). By varying parameters, we show in Figs. 3(c) and 3(d) that the time-averaged emf is linear with the external field and the current. Also, we found the average emf is ohmic because the emf is proportional to the length of the wire (not shown).

The emf predicted above could be experimentally measured. For example, we find that the averaged emf is about 0.1 mV across a 4 μm long permalloy wire with the current density $4\times10^{9}\mathrm{A/cm^2}$, $P=0.7$, $M_s=800$ emu/cc and the resistivity $\rho=20$ $\mu\Omega$ cm; this emf is about 0.3% of the total applied voltage.

ACKNOWLEDGMENTS

This work was partially supported by NSF (Grant No. DMR-0704182) and DOE (Grant No. DE-FG02-06ER46307).

[1] J. C. Slonczewski, J. Magn. Magn. Mater. **159**, L1 (1996).
[2] L. Berger, Phys. Rev. B **54**, 9353 (1996).
[3] M. Tsoi, A. G. M. Jansen, J. Bass, W.-C. Chiang, M. Seck, V. Tsoi, and P. Wyder, Phys. Rev. Lett. **80**, 4281 (1998); M. Tsoi, A. G. M. Jansen, J. Bass, W.-C. Chiang, V. Tsoi, and P. Wyder, Nature (London) **406**, 46 (2000).
[4] J. Z. Sun, J. Magn. Magn. Mater. **202**, 157 (1999).
[5] E. B. Myers, D. C. Ralph, J. A. Katine, R. N. Louie, and R. A. Buhrman, Science **285**, 867 (1999); S. M. Rezende, F. M. de Aguiar, M. A. Lucena, and A. Azevedo, Phys. Rev. Lett. **84**, 4212 (2000).
[6] J. Grollier, P. Boulenc, V. Cros, A. Hamzić, A. Vaurès, A. Fert, and G. Faini, Appl. Phys. Lett. **83**, 509 (2003).
[7] Y. Ji, C. L. Chien, and M. D. Stiles, Phys. Rev. Lett. **90**, 106601 (2003).
[8] B. Ozyilmaz, A. D. Kent, J. Z. Sun, M. J. Rooks, and R. H. Koch, Phys. Rev. Lett. **93**, 176604 (2004).
[9] S. S. P. Parkin, M. Hayashi, and L. Thomas, Science **320**, 190 (2008); M. Hayashi, L. Thomas, R. Moriya, C. Rettner, and S. S. P. Parkin, *ibid.* **320**, 209 (2008).
[10] C. Chappert, A. Fert, and F. N. Van Dau, Nat. Mater. **6**, 813 (2007).
[11] S. Laribi, V. Cros, M. Munoz, J. Grollier, A. Hamzić, C. Deranlot, and A. Fert, Appl. Phys. Lett. **90**, 232505 (2007).
[12] M. Kläui, P.-O. Jubert, R. Allenspach, A. Bischof, J. A. C. Bland, G. Faini, U. Rüdiger, C. A. F. Vaz, L. Vila, and C. Vouille, Phys. Rev. Lett. **95**, 026601 (2005).
[13] G. S. D. Beach, C. Knutson, C. Nistor, M. Tsoi, and J. L. Erskine, Phys. Rev. Lett. **97**, 057203 (2006).
[14] J. Shibata, G. Tatara, and H. Kohno, Phys. Rev. Lett. **94**, 076601 (2005).
[15] Y. Nakatani, J. Shibata, G. Tatara, H. Kohno, A. Thiaville, and J. Miltat, Phys. Rev. B **77**, 014439 (2008).
[16] Ya. B. Bazaliy, B. A. Jones, and S.-C. Zhang, Phys. Rev. B **57**, R3213 (1998).
[17] J. Fernández-Rossier, M. Braun, A. S. Núñez, and A. H. MacDonald, Phys. Rev. B **69**, 174412 (2004).
[18] Z. Li, J. He, and S. Zhang, J. Appl. Phys. **97**, 10C703 (2005); **99**, 08Q702 (2006).
[19] S. M. Rezende, F. M. de Aguiar, and A. Azevedo, Phys. Rev. B **73**, 094402 (2006).
[20] I. Y. Korenblit, Phys. Rev. B **77**, 100404(R) (2008).
[21] S. Zhang and Z. Li, Phys. Rev. Lett. **93**, 127204 (2004).
[22] A. Thiaville, Y. Nakatani, J. Miltat, and Y. Suzuki, Europhys. Lett. **69**, 990 (2005).
[23] S. E. Barnes and S. Maekawa, Phys. Rev. Lett. **98**, 246601 (2007).
[24] H. Kohno, G. Tatara, and J. Shibata, J. Phys. Soc. Jpn. **75**, 113706 (2006).
[25] Y. Tserkovnyak, A. Brataas, and G. E. W. Bauer, J. Magn. Magn. Mater. **320**, 1282 (2008).
[26] W. M. Saslow, Phys. Rev. B **76**, 184434 (2007).
[27] R. A. Duine, Phys. Rev. B **77**, 014409 (2008).
[28] S. A. Yang, D. Xiao, and Q. Niu, arXiv:0709.1117 (unpublished).
[29] A. Brataas, Y. Tserkovnyak, G. E. W. Bauer, and B. I. Halperin, Phys. Rev. B **66**, 060404(R) (2002).